Contribution of Low-Cost Sensor Measurements to the Prediction of $PM_{2.5}$ Levels: A Case Study in Imperial County, California, USA

Jianzhao Bi[1], Jennifer Stowell[1], Edmund Y.W. Seto[2], Paul B. English[3], Mohammad Z. Al-Hamdan[4], Patrick L. Kinney[5], Frank R. Freedman[**,6], and Yang Liu[*,1]

[1]Department of Environmental Health, Emory University, Rollins School of Public Health, Atlanta, GA 30322, USA
[2]Department of Environmental & Occupational Health Sciences, University of Washington, Seattle, WA 98195, USA
[3]California Department of Public Health, Richmond, CA 94804, USA
[4]Universities Space Research Association, NASA Marshall Space Flight Center, Huntsville, AL 35808, USA
[5]Department of Environmental Health, Boston University, School of Public Health, Boston, MA 02118, USA
[6]Department of Meteorology and Climate Science, San Jose State University, San Jose, CA 95192, USA

Highlights:

- Ground-level $PM_{2.5}$ was assessed with low-cost, regulatory, and satellite data
- Low-cost sensor measurements contributed to improved modeling performance
- Reasonable $PM_{2.5}$ spatial details were revealed due to abundant low-cost data
- Remaining uncertainty in calibrated low-cost data still affected modeling precision

Abstract: Regulatory monitoring networks are often too sparse to support community-scale $PM_{2.5}$ exposure assessment while emerging low-cost sensors have the potential to fill in the gaps. To date, limited studies, if any, have been conducted to utilize low-cost sensor measurements to improve $PM_{2.5}$ prediction with high spatiotemporal resolutions based on statistical models. Imperial County in California is an exemplary region with sparse Air Quality System (AQS) monitors and a community-operated low-cost network entitled Identifying Violations Affecting Neighborhoods (IVAN). This study aims to evaluate the contribution of IVAN measurements to the quality of $PM_{2.5}$ prediction. We adopted the Random Forest algorithm to estimate daily $PM_{2.5}$ concentrations at a 1-km spatial resolution using three different $PM_{2.5}$ datasets (AQS-only, IVAN-only, and AQS/IVAN combined). The results show that the integration of low-cost sensor measurements is an effective way to significantly improve the quality of $PM_{2.5}$ prediction with an increase of cross-validation (CV) R^2 by ~0.2. The IVAN measurements also contributed to the increased importance of emission source-related covariates and more reasonable spatial patterns of $PM_{2.5}$. The remaining uncertainty in the calibrated IVAN measurements could still cause apparent outliers in the prediction model, highlighting the need for more effective calibration or integration methods to relieve its negative impact.

Keywords: Low-cost sensor; Satellite AOD; Random forest; Measurement uncertainty

Corresponding Authors:

*Emory University, Rollins School of Public Health, 1518 Clifton Road NE, Atlanta, GA 30322, USA. E-mail: yang.liu@emory.edu.

**San Jose State University, Department of Meteorology and Climate Science, One Washington Square, San Jose, CA 95192, USA. E-mail: frank.freedman@sjsu.edu.

This is an accepted manuscript by Environmental Research (Volume 180, January 2020, 108810). Please refer to https://doi.org/10.1016/j.envres.2019.108810 for the formal publication.

1 Introduction

Fine particulate matter with an aerodynamic diameter less than or equal to 2.5 micrometers ($PM_{2.5}$) has been contributing to a growing disease burden worldwide, causing premature mortalities and a variety of morbidities including cardiovascular, cerebrovascular, and respiratory diseases (Bose et al., 2015; Burnett et al., 2014; Madrigano et al., 2013; Sorek-Hamer et al., 2016). Traditionally, ambient $PM_{2.5}$ exposure assessments have mainly relied on measurements from ground monitoring stations. However, as regulatory monitoring is designed to support compliance with ambient air quality standards (Hall et al., 2014), it lacks spatial coverage to reflect detailed $PM_{2.5}$ variations at the community level. Even in the United States, more than 70% of counties do not have regulatory $PM_{2.5}$ monitoring so far. Exposure misclassification due to insufficient coverage of regulatory $PM_{2.5}$ monitoring can significantly bias the estimated health impacts of $PM_{2.5}$ (Zeger et al., 2000).

Over the past decade, satellite aerosol remote sensing has emerged as a useful tool to extend the coverage of ground $PM_{2.5}$ monitoring (Bi et al., 2019; Di et al., 2016; Hu et al., 2017; Kloog et al., 2011; Ma et al., 2016; Xiao et al., 2017). Instruments aboard polar-orbiting satellites such as the Moderate Resolution Imaging Spectroradiometer (MODIS) and the Multi-angle Imaging SpectroRadiometer (MISR) have been supplying Aerosol Optical Depth (AOD) retrievals with global coverage. AOD is a measure of aerosol extinction of the solar beam along the entire vertical atmospheric column. The relationship of AOD to ground-level $PM_{2.5}$ depends on factors such as aerosol vertical profile, water content, size distribution, and composition (Paciorek et al., 2008; van Donkelaar et al., 2010). Since many of these factors are not available at large spatial scales, strategies such as statistical models (Hu et al., 2014; Paciorek et al., 2008; Xiao et al., 2017) and chemical transport model (CTM)-based scaling approaches (Liu et al., 2004; van Donkelaar et al., 2010) have been developed to recover the AOD-$PM_{2.5}$ relationship. Statistical models have been widely used at urban to national scales due to their excellent performance and ability to yield high-resolution predictions (Chu et al., 2016). Recently, there is a growing trend of using non-parametric machine learning models such as artificial neural networks (Di et al., 2016; Zou et al., 2015) and random forests (Bi et al., 2019; Brokamp et al., 2018; Hu et al., 2017) to better estimate $PM_{2.5}$ based on AOD and other covariates. With these methods, spatiotemporally complete estimates of $PM_{2.5}$ levels have been able to be generated (Di et al., 2016; Just et al., 2015; Ma et al., 2016; Wang et al., 2017).

Sufficient and well-distributed ground measurements are critical to the successful development of statistical $PM_{2.5}$ models. An unevenly distributed network may limit the use of statistical models and the quality of models may significantly decrease as the number of ground measurements reduces (Geng et al., 2018a). The validation of prediction results may become unreliable when ground measurements are sparse and the actual quality of predictions is even unknown in the areas without ground measurements. The requirements on ground stations are stricter when $PM_{2.5}$ has significant variations at a fine scale especially in the areas with complex terrain and many local sources (Saide et al., 2011; van Donkelaar et al., 2006, 2010) such as Western United States (Geng et al., 2018b; van Donkelaar et al., 2006). Additionally, as regulatory monitoring primarily aims to examine the compliance of air quality standards rather than assess exposure, existing ground stations are unlikely to represent concentrations where sensitive subpopulations reside. This issue can further limit the utility of regulatory monitoring data in community-level exposure assessment.

Recently emerged low-cost $PM_{2.5}$ sensors have the potential to fill in the gaps of regulatory $PM_{2.5}$ monitoring and to overcome the limitations of statistical models based solely on regulatory measurements. With the features of lower instrument cost, ease of use, and portability (Jiao et al., 2016; Snyder et al., 2013), low-cost $PM_{2.5}$ sensors can be densely deployed by researchers, grass-roots organizations, and citizen scientists. For example, a commercial low-cost PM monitoring network established in 2015, PurpleAir (`https://www.purpleair.com/`), has more than 7,000 nodes worldwide with a growth rate of ~30 per day (Morawska et al., 2018). The emergence of low-cost sensors has been shifting the paradigm of air pollution monitoring from being based solely on regulatory networks to mixed networks consisting of both regulatory and low-cost monitors (Snyder et al., 2013), and from being conducted by government agencies to increasingly commercial/crowd-funded projects (Morawska et al., 2018; Snyder et al., 2013). As most of the low-cost $PM_{2.5}$ sensors use optical light scattering to count particles and convert them to mass concentrations, they tend to have lower accuracy and precision than regulatory monitors (Xu, 2001). However, growing efforts have been made to calibrate low-cost $PM_{2.5}$ measurements in both laboratory and ambient settings (Broday

et al., 2017; Cao and Thompson, 2017; Castell et al., 2017; Holstius et al., 2014; Kelly et al., 2017; Wang et al., 2015). With a significant amount and a high growth rate, low-cost sensors are expected to shed light on more detailed spatial variations of $PM_{2.5}$ at finer scales.

To date, limited studies have focused on using low-cost sensor measurements to improve $PM_{2.5}$ prediction with high spatiotemporal resolutions. This study aimed to evaluate the contribution of low-cost sensor measurements to the estimation of $PM_{2.5}$ levels in the areas where sparse regulatory monitors alone cannot support reliable predictions. This case study focused on Imperial County, California, an exemplary region with $PM_{2.5}$ pollution intermittently exceeding the U.S. air quality standard (35 $\mu g/m^3$ for 24-hour $PM_{2.5}$ and 12 $\mu g/m^3$ for annual $PM_{2.5}$) especially near the U.S.-Mexico border. The $PM_{2.5}$ pollution is also associated with critical health issues which promoted a community-based low-cost monitoring network designed to address public concerns about the ability of regulatory monitors to reflect true pollution in local communities (English et al., 2017). Based on both regulatory and low-cost measurements in Imperial County, daily $PM_{2.5}$ predictions with a 1-km resolution were generated by the Random Forest algorithm with satellite AOD and relevant covariates. The reliability of $PM_{2.5}$ predictions before and after the integration of low-cost $PM_{2.5}$ measurements were investigated. The limitation of low-cost $PM_{2.5}$ measurements caused by their remaining uncertainty and the future perspectives of better utilizing these measurements were also discussed.

2 Data and Methods

2.1 Study Domain

Imperial County is located in the southern part of the U.S. state of California, bordering the Mexican state of Baja California. This county has $PM_{2.5}$ levels frequently exceeding the U.S. air quality standard with a high rate of childhood asthma-related emergency room visits (CEHTP, 2018). The desert on its west side, the dry lake bed of a saline lake (the Salton Sea) where an exposed playa is contributing to dust levels (Parajuli and Zender, 2018), and the transboundary pollution have caused substantial variability of $PM_{2.5}$ levels in different communities of the county (English et al., 2017). However, by 2017, there were only three U.S. Environmental Protection Agency (EPA) Air Quality System (AQS) stations within the county and three additional near the county that spans over 40,000 square kilometers (Figure 1). To meet the request of local communities about more extensive $PM_{2.5}$ measurements, a low-cost $PM_{2.5}$ monitoring network, Identifying Violations Affecting Neighborhoods (IVAN), has been established by a community-engaged research project (English et al., 2017). As of 2017, the IVAN had built ~40 community $PM_{2.5}$ monitoring sites throughout the county.

In this study, the AQS and calibrated IVAN measurements in Imperial County were served as ground truth for $PM_{2.5}$ prediction. Figure 1 shows the study domain with the locations of AQS and IVAN sites. The study domain includes a 50-km buffer beyond the county border to include nearby AQS stations and better illustrate the patterns of transboundary pollution. Within the study domain, there were 6 AQS stations and 39 IVAN sensors. A 1-km modeling grid covers the study domain, which totals 41,344 grid cells. The modeling period was from September 2016 to November 2017 to be consistent with the time span of available calibrated IVAN $PM_{2.5}$ measurements.

2.2 $PM_{2.5}$ Measurements

Regulatory $PM_{2.5}$ measurements were provided by the U.S. EPA AQS (`https://www.epa.gov/outdoor-air-quality-data`). Low-cost $PM_{2.5}$ measurements were provided by the IVAN air monitoring system (`https://www.ivan-imperial.org/`). The IVAN low-cost PM sensor was a modified version of particle counter Dylos 1700 (Dylos Corporation, Riverside, California). Raw particle counts from Dylos sensors were calibrated and converted to hourly $PM_{2.5}$ mass concentrations using the conversion equation developed by Carvlin et al. (2017). After a validation with additional collocated reference instruments, Carvlin et al. (2017) found that the conversion accuracy was moderate to high with R^2 values ranging from 0.35 to 0.81 with an average of 0.59. In this study, hourly IVAN $PM_{2.5}$ concentrations were further averaged into daily means (Section 1, Supplementary Material). Negative $PM_{2.5}$ measurements from both networks caused by

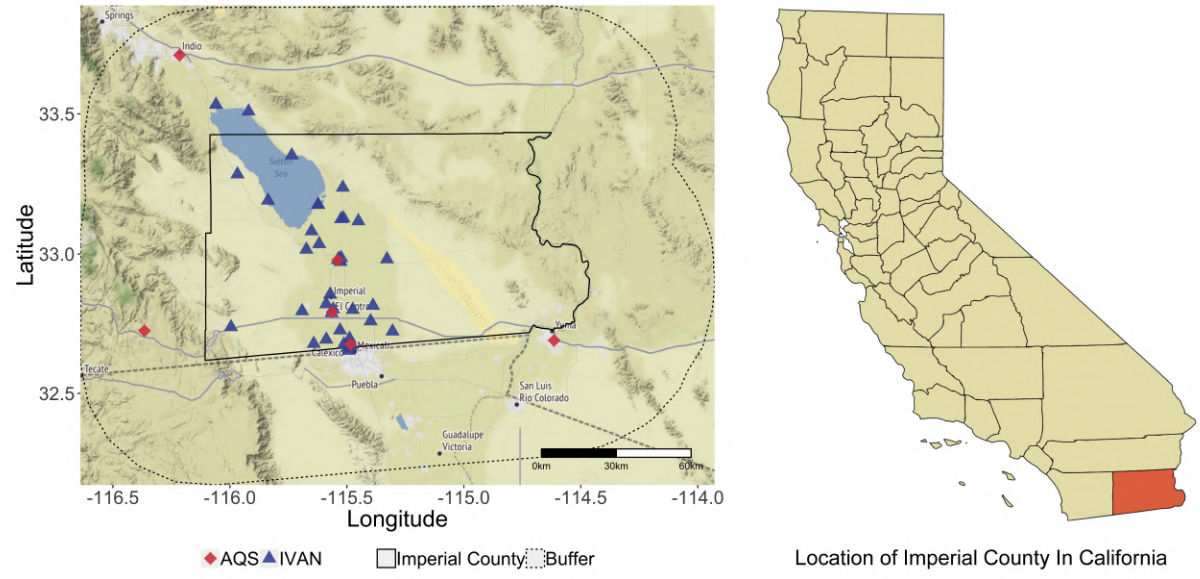

Figure 1: Study domain (latitude: [32.2°N, 33.9°N]; longitude: [113.9°W, 116.6°W]). Imperial County is part of the Southern California border region contiguous to the Mexican state of Baja California. The area surrounded by the dashed line is a buffer mainly used to better reflect transboundary pollution.

random errors in a clean environment (approaching 0 $\mu g/m^3$) were retained to prevent systematic biases (Paciorek et al., 2008).

2.3 AOD Retrievals

The Multi-Angle Implementation of Atmospheric Correction (MAIAC) is an advanced MODIS AOD product with global coverage at a 1-km spatial resolution on a daily basis (MCD19, https://modis-land.gsfc.nasa.gov/MAIAC.html). In order to reflect daytime changes of AOD, Terra (descending node at 10:30 a.m. local time) and Aqua (ascending node at 1:30 p.m. local time) AOD served as two separate variables in the prediction models. According to the quality assessment parameters within MAIAC, the AOD retrievals with poor quality were filtered out. We followed the approach proposed by Bi et al. (2019) to fill in missing AOD values, in which Random Forest models with AOD-related predictors were established at the daily level (Section 2, Supplementary Material).

2.4 Meteorological Data

Cloud fraction, as the percentage of cloud cover, is an important covariate in AOD gap-filling since most of the missing AOD data were caused by the existence of cloud in Imperial County. In this study, satellite-observed cloud fractions were obtained from the MODIS Level-2 Cloud product (MOD06_L2/MYD06_L2, https://modis.gsfc.nasa.gov/). Other meteorological variables were obtained from the High-Resolution Rapid Refresh (HRRR) (https://rapidrefresh.noaa.gov/hrrr/), a National Oceanic and Atmospheric Administration real-time 3-km resolution updated atmospheric model. The HRRR meteorological parameters include 2-meter temperature and specific humidity, planetary boundary layer (PBL) height, sensible heat net flux, frictional velocity, and 10-meter wind direction and speed. These HRRR fields were from the initial forecast hour of operational hourly 18-hour forecast runs. The fields were obtained from the University of Utah Center for High-Performance Computing real-time HRRR archive (http://hrrr.chpc.utah.edu/) (Blaylock et al., 2017).

2.5 Land-Use Data

The land-use parameters include 1) the Advanced Spaceborne Thermal Emission and Reflection Radiometer (ASTER) Global Digital Elevation at a 1 arc-second (∼30 m) resolution (https://asterweb.jpl.nasa.gov/gdem.asp), 2) LandScan ambient population in 2016 at a 900-m resolution (https://web.ornl.gov/sci/landscan/), 3) Normalized Difference Vegetation Index (NDVI) from the MODIS vegetation indices (MOD13/MYD13) at a 500-m resolution, 4) the distance to the nearest major road computed from Topologically Integrated Geographic Encoding and Referencing (TIGER)/Line Geodatabases of the U.S. Census Bureau and DIVA-GIS (http://www.diva-gis.org/), 5) 0 – 10 cm soil moisture from the North American Land Data Assimilation System (NLDAS) Noah Land Surface Model at a 0.125-degree resolution, 6) 8-day land surface temperature from the MODIS land products (MOD11A2/MYD11A2) at a 1-km resolution, and 7) the percentages of grassland and water body calculated from GlobCover V2.3 land cover product (European Space Agency, http://due.esrin.esa.int/page_globcover.php).

2.6 $PM_{2.5}$ Prediction Models

To evaluate the contribution of low-cost sensor measurements to the quality of $PM_{2.5}$ estimates, three models with different types of dependent variables were built: 1) the AQS-only model, 2) the IVAN-only model, and 3) the AQS/IVAN-combined model. In the first two models, either AQS or IVAN $PM_{2.5}$ measurements were used as the dependent variable. In the third model, both AQS and IVAN $PM_{2.5}$ measurements were combined. Since the IVAN measurements had been calibrated and validated with collocated reference-grade measurements (Carvlin et al., 2017), we treated these measurements as ground truth and simply merged them with AQS measurements. Three models shared the same set of independent variables shown in Table 1. The models were based on the Random Forest (RF) algorithm. RF is an "ensemble learning" method generating a number of decision trees and aggregating the regression results from these trees (Breiman, 2001). Other statistical models such as the multi-stage LME-GAM (Linear Mixed Effects-Generalized Additive Model) (Xiao et al., 2017), XGBoost (Xiao et al., 2018), and artificial neural networks (Di et al., 2016) were also tested in the pilot stage of this study, but RF was able to generate the most stable and accurate predictions. The number of decision trees in the forest (n_{tree}) and the number of predictors randomly tried at each split (m_{try}) are two major hyperparameters of RF. In this study, n_{tree} was set to be 1,000 to guarantee the stability of predictions and m_{try} was tuned with cross-validation (CV) and determined to be 6. The prediction model could generate spatiotemporally continuous $PM_{2.5}$ estimates with a 1-km resolution at the daily level. The evaluation of the models was conducted with 10-fold CV (*i.e.*, dropping 10% of $PM_{2.5}$ observations). Evaluation metrics include CV R^2 and root-mean-square error (RMSE). The 10-fold CV consists of overall, spatial, and temporal CVs (Xiao et al., 2017). 10-fold spatial/temporal CV creates validation sets according to the locations/Julian days of measurements (*i.e.*, dropping 10% of all locations/days of observations). Spatial and temporal CVs demonstrate model predictability at different locations and times than the observations used to train the model. Additionally, RF-specific "permutation accuracy importance" (Breiman, 2001) was used to reflect the importance of covariates in the prediction model. This importance measure is estimated according to the decrease of prediction accuracy when randomly permuting the "out-of-bag" sample of the targeting variable (Liaw and Wiener, 2002).

The independent variables were determined based on the $PM_{2.5}$ emission features in Imperial County. As fugitive dust was emitted from the dry lake bed of the Salton Sea (King et al., 2011; Parajuli and Zender, 2018), we used wind speed and direction, surface soil moisture, and land surface temperature to reflect the properties of dust emission jointly. $PM_{2.5}/PM_{10}$ ratio, *i.e.*, the percentage of $PM_{2.5}$ in PM_{10}, was found to be a critical predictor with a high RF variable importance value. This predictor has rarely been considered in previous studies regarding $PM_{2.5}$ prediction. As several $PM_{2.5}$ emission sources in Imperial County also emitted a large amount of PM_{10} (*e.g.*, dust emissions) (Chow et al., 2000; Parajuli and Zender, 2018), this ratio could help to modify the relationship between AOD and $PM_{2.5}$. Another ancillary covariate, $PM_{2.5}$ convolutional layer, was created following Hu et al. (2017) who showed that this variable could improve the accuracy of $PM_{2.5}$ prediction by considering $PM_{2.5}$ spatial autocorrelation.

Table 1: Independent variables in three $PM_{2.5}$ prediction models (s - spatially varying; t - temporally varying).

Prediction Variables	
MAIAC AOD	**$PM_{2.5}$-ancillary variables**
Gap-filled Terra/Aqua $AOD_{(s,t)}$	$PM_{2.5}$ convolutional $layer_{(s,t)}$
Land-use variables	$PM_{2.5}/PM_{10}$ $ratio_{(t)}$
$Elevation_{(s)}$	**Meteorological variables**
$Population_{(s)}$	2-meter $temperature_{(s,t)}$
$NDVI_{(s,t)}$	2-meter specific $humidity_{(s,t)}$
Nearest distance to $road_{(s)}$	Planetary boundary layer $height_{(s,t)}$
0 – 10 cm soil $moisture_{(s,t)}$	Sensible heat net $flux_{(s,t)}$
Land surface $temperature_{(s,t)}$	Frictional $velocity_{(s,t)}$
Percentage of $grassland_{(s)}$	10-meter wind $direction_{(s,t)}$
Percentage of water $body_{(s)}$	10-meter wind $speed_{(s,t)}$

3 Results

3.1 Summary Statistics and Modeling Performance

Within the study domain, AQS $PM_{2.5}$ measurements had a mean of 8.55 $\mu g/m^3$ with an interquartile range (IQR) of 5.80 $\mu g/m^3$ (25% and 75% percentiles: [5.00 $\mu g/m^3$, 10.80 $\mu g/m^3$]). IVAN $PM_{2.5}$ measurements had a mean of 7.44 $\mu g/m^3$ with an IQR of 5.28 $\mu g/m^3$ (25% and 75% percentiles: [3.65 $\mu g/m^3$, 8.93 $\mu g/m^3$]). AQS measured slightly higher $PM_{2.5}$ concentrations ($\sim$1 $\mu g/m^3$) than IVAN during the study period. The performance of three $PM_{2.5}$ prediction models (AQS-only, IVAN-only, and AQS/IVAN) was summarized in Table 2. Figure 2 shows cross-validation's scatter plots of the models. Six AQS stations only provided 1,617 samples and the overall 10-fold CV R^2 of the AQS-only model was 0.53. The spatial CV R^2 of the model dropped to 0.24, indicating that the AQS measurements alone could not support reliable prediction of $PM_{2.5}$ spatial patterns. In contrast, 39 IVAN sensors provided 11,965 samples and the IVAN-only model had an overall 10-fold CV R^2 of 0.75. The spatial and temporal CV R^2 values of this model (0.64 and 0.70, respectively) were slightly lower than the overall CV R^2 but still significantly higher than those of the AQS-only model. All three models had similar RMSE values ranged from 3.71 to 3.76 $\mu g/m^3$. This was a reasonable value consistent with Hu et al. (2017) who had a regional RMSE of 3.32 $\mu g/m^3$ in the western climate region (including California and Nevada) in their U.S. national $PM_{2.5}$ prediction model for the year of 2011.

Apart from the regular CV, the AQS measurements were also used as a test set to validate the IVAN-only model. This validation was designed to examine to what extent the IVAN-based predictions could agree with AQS measurements and whether the IVAN measurements alone could support a reliable $PM_{2.5}$ prediction model. The validation showed an R^2 of 0.43 between the AQS measurements and the IVAN-based predictions. This R^2 value is lower than the CV R^2 of the AQS-only model, 0.53. The decreased R^2 indicates that the IVAN-based predictions still deviated from actual $PM_{2.5}$ levels to a certain degree. Given the moderate to high correlation between calibrated IVAN measurements and collocated reference observations (Carvlin et al., 2017), we infer that the deviation may be due to the uncertainty in calibrated IVAN measurements which was not able to be reduced (the remaining uncertainty of IVAN hereinafter). Less representative monitor siting of IVAN could be another potential reason for the lower agreement (Geng et al., 2018a). This validation emphasized the importance and necessity of keeping high-quality regulatory measurements in $PM_{2.5}$ prediction even though they are temporally less-frequent and spatially sparser.

After combining the AQS and IVAN observations, the modeling performance had a slight decrease with overall, spatial, and temporal CV R^2 values of 0.73, 0.63, and 0.70, respectively. Again, we infer that the decreased performance could be caused by the remaining uncertainty of IVAN. This uncertainty could be seen in the scatter plot of the IVAN-only model as there were more apparent outliers deviating from the 1:1 line (Figure 2(b)). The remaining uncertainty again indicates that good fitting performance of the IVAN-

only model did not necessarily mean an accurate representation of actual $PM_{2.5}$ levels. We considered the AQS/IVAN model as the optimal model because it incorporated both detailed spatial patterns of $PM_{2.5}$ provided by IVAN and additional accurate $PM_{2.5}$ constraint provided by AQS.

Table 2: The performance of three models with overall, spatial, and temporal CV R^2 and RMSEs.

Model	N	Overall CV R^2	Spatial CV R^2	Temporal CV R^2	RMSE
AQS-Only	1,617	0.53	0.24*	0.55	3.76 $\mu g/m^3$
IVAN-Only	11,965	0.75	0.64	0.7	3.71 $\mu g/m^3$
AQS/IVAN	12,902	0.73	0.63	0.7	3.72 $\mu g/m^3$

*6-fold (leave-one site-out) spatial CV as there were only 6 AQS stations

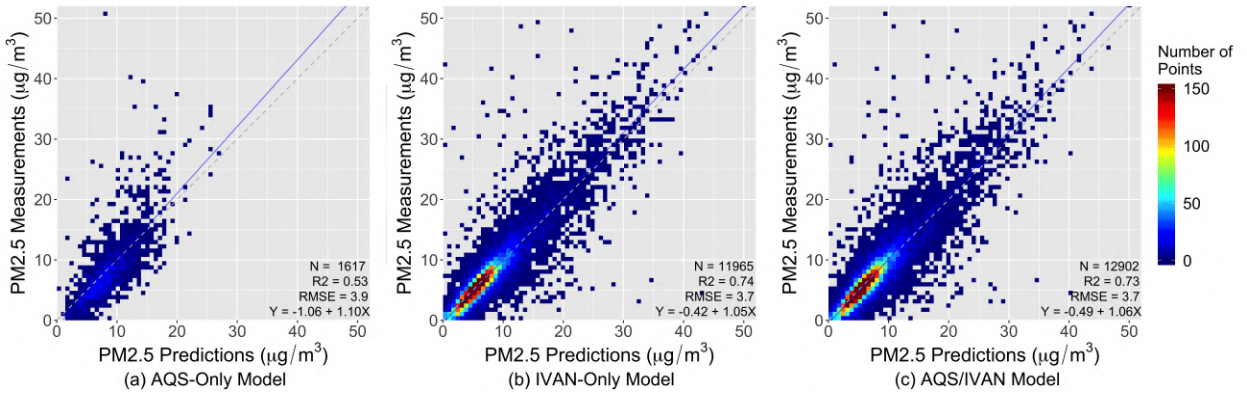

Figure 2: 10-fold CV scatter plots of three models: (a) AQS-only model, (b) IVAN-only model, and (c) AQS/IVAN model.

3.2 Analyses with $PM_{2.5}$ Predictions

Statistical metrics such as CV R^2 and RMSE only reflect model predictability at monitoring locations. Within our study domain, ground monitors were not evenly distributed, leaving large areas in the southern and eastern parts uncovered (Figure 1). This uneven distribution reduced the effectiveness of the statistical metrics. Due to the lack of reliable references regarding $PM_{2.5}$ pollution in Imperial County from other sources, we focused more on analyzing the features of prediction results to examine the quality of $PM_{2.5}$ estimates and the contribution of IVAN measurements to the prediction.

Figure 3 shows the averaged distributions of daily $PM_{2.5}$ estimates during the study period. The AQS-based distribution emphasized $PM_{2.5}$ pollution near major roads by showing spatially resolved $PM_{2.5}$ concentrations on the road network (Figure 3(a)). This road-specific feature may be related to a fact that the AQS stations were relatively close to the major roads in the study domain. The mean distance from 6 AQS stations to the major roads was ~600 m and the maximum distance was ~2,000 m. On the contrary, the IVAN sites had a mean distance of ~7,600 m with a maximum longer than 10,000 m. The distance-to-road of the IVAN sites also distributed more evenly within its range compared to which of the AQS stations. The lack of AQS stations away from the major roads reduced the ability of AQS to reflect off-road pollution. The $PM_{2.5}$ estimates derived from the IVAN-only model (Figure 3(b)) and the AQS/IVAN model (Figure 3(c)) did not show road-specific patterns but smoother $PM_{2.5}$ distributions. This result indicates that more extensively distributed IVAN measurements could better reflect off-road pollution sources.

Apart from more credible $PM_{2.5}$ spatial patterns, the contribution of IVAN measurements can also be reflected by the importance of pollution source-related covariates in the models. Table 3 shows the top-10 important covariates determined by the RF algorithm in three models. In the AQS-only model, temporally varying parameters such as meteorological parameters (PBL height, wind speed and direction, and sensible

heat net flux) dominated the most important covariates. This feature reflects that sparse AQS measurements well captured temporal patterns of $PM_{2.5}$ but provided limited information regarding the spatial distribution of $PM_{2.5}$, which echoes the low spatial CV R^2 in the AQS-only model (Table 2). On the contrary, time-invariant and source-related parameters, especially population, elevation, the nearest distance to road, and the percentage of grassland, had increased importance in the IVAN-only and AQS/IVAN models. The increased importance of these source-related covariates indicates that spatially denser IVAN measurements resolved more spatial information of $PM_{2.5}$ in different geographical environments associated with varying pollution sources.

The $PM_{2.5}$ spatial patterns derived from the AQS/IVAN model can be explained properly with the emission sources in Imperial County, and these patterns are also consistent with the coarser distributions observed in previous studies (Di et al., 2016; Hu et al., 2017; Parajuli and Zender, 2018). In the AQS/IVAN-based estimates, the highest $PM_{2.5}$ levels occurred on the U.S.-Mexico border, especially in the border cities Calexico and Mexicali where annual $PM_{2.5}$ level exceeded the U.S. air quality standard of 12 $\mu g/m^3$ during the study period. This transboundary $PM_{2.5}$ hot-spot was also shown in Hu et al. (2017) who estimated $PM_{2.5}$ levels in the contiguous U.S. at a 12-km resolution. This hot-spot was not captured by the AQS-based predictions because of limited AQS stations located in similar geographical environments (only one station near the border). Elevated $PM_{2.5}$ levels also occurred on the desert and exposed playa over the southwest shore of the Salton Sea. These high $PM_{2.5}$ levels were likely to be associated with dust emissions in the areas, which is supported by Parajuli and Zender (2018) who suggested that newly exposed playa of the Salton Sea had contributed to a large amount of dust emissions in the southwest side of the lake. Brawley, a city in the south of the Salton Sea, showed a moderate $PM_{2.5}$ hot-spot with mean $PM_{2.5}$ concentrations ranged from 7.1 to 7.8 $\mu g/m^3$. The elevated $PM_{2.5}$ might be related to the significant cattle and feed industry in the city as the pulverized manure and animal activity in cattle feedlots may contribute to the emissions of ammonia and nitric oxide that subsequently lead to the formation of secondary $PM_{2.5}$ (Rogge et al., 2006; Wilson et al., 2002).

It should be noted that although the $PM_{2.5}$ patterns derived from the AQS/IVAN model (Figure 3(c)) were similar to which of the IVAN-only model (Figure 3(b)) due to the dominance of IVAN measurements, the additional AQS measurements still led to noticeable changes. For example, the lower-left AQS station outside the county's border resulted in decreased $PM_{2.5}$ levels in its neighboring broad, mountainous areas covered by dense vegetation. The lower $PM_{2.5}$ levels could be explained by the reduced ventilation and transport of pollutants affected by topography and less residential emissions associated with fewer people living in the region (Chow et al., 2006). This result again shows the importance of keeping AQS measurements in the prediction model despite their smaller sample size. Figure S1 shows the $PM_{2.5}$ distributions by season. In spring and summer, $PM_{2.5}$ had higher background levels and lower peak levels due to the atmospheric conditions favorable for diffusion. In contrast, $PM_{2.5}$ tended to be accumulated in winter due to stagnant weather conditions.

Table 3: Top-10 important covariates determined by the RF algorithm in three prediction models. The bold font highlights the time-invariant and source-related covariates with the increased importance after the addition of IVAN.

Rank	AQS-Only	IVAN-Only	AQS/IVAN
1	$PM_{2.5}$ convolutional layer	$PM_{2.5}$ convolutional layer	$PM_{2.5}$ convolutional layer
2	PBL height	PBL height	**Population**
3	NDVI	**Population**	**Elevation**
4	0 – 10 cm soil moisture	**Elevation**	PBL height
5	10-meter wind direction	$PM_{2.5}/PM_{10}$ ratio	NDVI
6	2-meter specific humidity	0 – 10 cm soil moisture	**Percentage of grassland**
7	10-meter wind speed	NDVI	$PM_{2.5}/PM_{10}$ ratio
8	Sensible heat net flux	**Nearest distance to road**	0 – 10 cm soil moisture
9	$PM_{2.5}/PM_{10}$ ratio	**Percentage of grassland**	**Nearest distance to road**
10	Frictional velocity	2-meter specific humidity	2-meter temperature

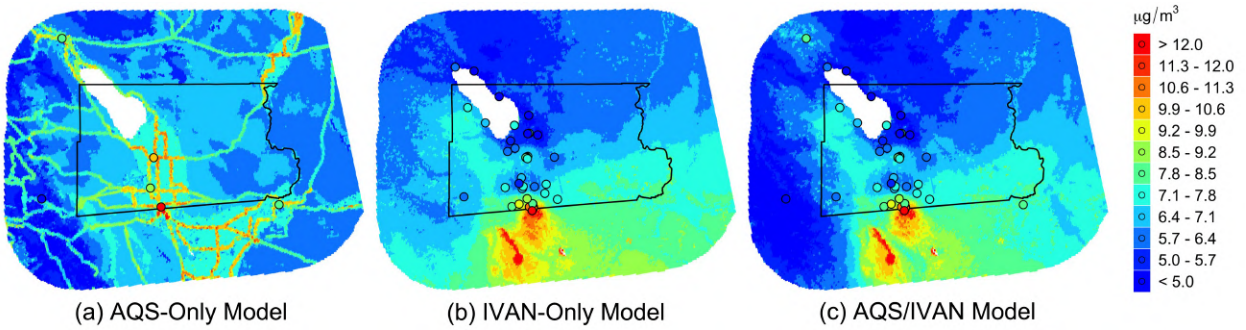

Figure 3: Mean $PM_{2.5}$ distributions for the period from September 2016 to November 2017 generated by three models: (a) AQS-only model, (b) IVAN-only model, and (c) AQS/IVAN model. The points show mean $PM_{2.5}$ concentrations at the AQS and IVAN stations during the period.

3.3 Impact of IVAN Remaining Uncertainty

Given the moderate to high agreement between IVAN and collocated reference measurements after calibration (Carvlin et al., 2017), we analyzed the prediction outliers to evaluate the influence of the remaining uncertainty of IVAN on the prediction accuracy. We defined an outlier as a prediction a factor of two greater or smaller than the corresponding measurement in cross-validation. As we kept negative $PM_{2.5}$ observations, the predictions with a reversed sign were also considered as outliers. Figure 4 shows the CV scatter plot the same as Figure 2(c) with outliers in different colors. There were 1,500 outliers among the total 12,902 predictions, in which 312 were underestimated and 1,188 were overestimated. Compared to previous $PM_{2.5}$ modeling efforts based solely on regulatory measurements (Ma et al., 2016; Xiao et al., 2017), this CV scatter plot has more apparent outliers. Figure S2 shows the frequencies of outliers in different grid cells and Figure S3 shows the relationships between the number of outliers and the number of total observations in a grid cell. We found that the outliers were randomly distributed without specific spatiotemporal patterns and the number of outliers was positively associated with the number of total observations in a grid cell. The results reflect that the remaining uncertainty of IVAN still had an evident influence on the predictions, which homogeneously affected the modeling accuracy. The only collocated AQS/IVAN site (Calexico-Ethel Site, located at the Calexico High School on East Belcher Street) in the study domain could not support comprehensive analyses of outliers, and it remains unknown that what the sources of these outliers were, how these sources were associated with the prediction accuracy, and why overestimated outliers dominated the prediction biases.

4 Discussion

Imperial County is an exemplary region for studying the effectiveness of low-cost PM measurements in the U.S. The PM ($PM_{2.5}$ and PM_{10}) pollution in this county frequently exceeds state and national air quality standards (CARB, 2017). Poor air quality, poverty, and a high unemployment rate are associated with severe health issues such as childhood asthma, which lead to increasing needs voiced by the local residents for a comprehensive and accurate display of air quality (English et al., 2017). During the development of the IVAN network, community members were involved in the study design and monitor siting, and the study community partner staff were trained in monitor assembly/troubleshooting and data transfer and analysis (Wong et al., 2018). The IVAN network is now community operated and maintained. Developed community capacity to run the low-cost network addresses the core of environmental health issues in this primarily Hispanic and monolingual area by providing neighborhood-level data on air quality and increasing local environmental health literacy (Garzón-Galvis et al., 2019).

In this study, we evaluated the contribution of IVAN to $PM_{2.5}$ prediction in Imperial County with complex local $PM_{2.5}$ sources and a sparse regulatory network. On the one hand, our results show that current AQS

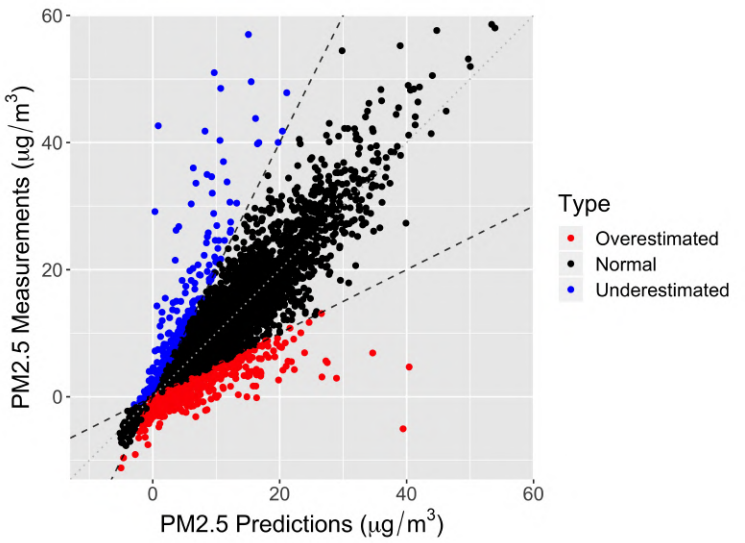

Figure 4: The 10-fold CV scatter plot of the AQS/IVAN model. The black dashed lines (with slopes of 2 and 0.5) divide the points into normal predictions and outliers. The points in red are overestimated outliers and the points in blue are underestimated outliers.

within the county could not support reliable $PM_{2.5}$ predictions as indicated by the significantly lower spatial CV R^2 of the AQS-only model compared to its overall CV R^2. The IVAN measurements, albeit noisier, were found to be able to serve as an effective supplement to the regulatory measurements to improve the modeling performance and prediction quality. Dense IVAN measurements also helped the predictions better resolve the spatial details of local pollution sources. On the other hand, although AQS was spatially sparser and temporally less-frequent than IVAN, its "gold-standard" measurements are still indispensable in $PM_{2.5}$ prediction. The necessity of keeping AQS was reflected by a lower validation R^2 when using the IVAN-only model to predict AQS measurements compared to the CV R^2 of the AQS-only model itself. The necessity was also reflected by more reasonable $PM_{2.5}$ prediction patterns around the AQS stations when combining AQS and IVAN. The combined AQS/IVAN predictions were in line with the coarser $PM_{2.5}$ patterns generated by the national-level models (Di et al., 2016; Hu et al., 2017), and the predicted $PM_{2.5}$ hot-spots can be properly explained by local $PM_{2.5}$ sources such as dust, transboundary, and agricultural pollution. Our analyses implicate that the combination of regulatory and low-cost sensor measurements is an effective way to improve the quality of $PM_{2.5}$ modeling and enable high-resolution $PM_{2.5}$ predictions in which they were impossible previously.

To date, the proposed calibration methods for low-cost $PM_{2.5}$ measurements have mainly focused on correcting systematic biases rather than reducing random errors commonly existing in the measurements (Carvlin et al., 2017; Holstius et al., 2014). In this study, we found that the remaining errors in the IVAN measurements, especially random errors, still had an apparent impact on the quality of $PM_{2.5}$ prediction after a calibration aiming to reduce the systematic biases (Carvlin et al., 2017). The influence of remaining uncertainty was reflected by obvious outliers in cross-validation scatters. As the uncertainty had a homogeneous effect on the predictions without obvious spatiotemporal patterns, it was difficult to pinpoint and remove inaccurate measurements. Additional studies with sufficient collocated regulatory/low-cost monitor pairs are needed for in-depth analyses regarding the low-cost sensor measurements' remaining uncertainty, *e.g.*, the sources of uncertainty and the quantitative influence of uncertainty on the prediction quality. The calibration methods aiming to reduce the random errors of low-cost sensor measurements, in addition to systematic biases, are also a potential way to improve the quality of $PM_{2.5}$ prediction.

Although spatiotemporally continuous $PM_{2.5}$ can be generated with CTMs, their simulations are difficult

to reflect detailed $PM_{2.5}$ pollution patterns at the community level. Specifically, the relatively coarse resolution and restricted emission information of CTMs limit their ability to characterize $PM_{2.5}$ distribution at small scales (Jerrett et al., 2005). Our study proved that the combination of dense and frequent low-cost sensor measurements, spatiotemporally continuous satellite AOD retrievals, and accurate reference-grade measurements is a possible solution to derive high-resolution $PM_{2.5}$ distribution details. Although the U.S. has one of the densest regulatory air quality monitoring networks in the world, only ∼2% of its counties have more active AQS $PM_{2.5}$ stations than Imperial County (with 3 active stations) (Figure 5(a)), and only ∼20% of the counties have a higher AQS station density than Imperial County (2.58 stations per 10,000 square kilometers) (Figure 5(b)). Accordingly, low-cost sensors have enormous potential to be applied to the vast regions in the U.S. and a large part of the world with sparse regulatory monitors to better support small-scale $PM_{2.5}$ prediction and help address $PM_{2.5}$-related health issues.

A major limitation of this study is the lack of reliable reference $PM_{2.5}$ measurements in Imperial County from other sources, which prevented quantitative assessments of our $PM_{2.5}$ estimates. However, many clues regarding the prediction models such as CV performance, variable importance, and spatial patterns of $PM_{2.5}$ estimates provided evidence that the integration of IVAN could lead to a better prediction quality in the region. Additional studies with sufficient reference measurements are needed to further prove the findings. The scale of the IVAN network is another potential limitation affecting the generalizability of our findings. As a county-level low-cost network with ∼40 sensors, which has been well maintained and operated by local communities, IVAN is less representative of other low-cost PM networks worldwide which may not be well maintained as such. A more general and extensive low-cost PM network is needed to further examine the effectiveness of our proposed $PM_{2.5}$ prediction framework and to test new methods regarding better utilization of low-cost sensor measurements in $PM_{2.5}$ prediction. PurpleAir, a worldwide commercial PM monitoring network built with low-cost sensors, is a potential one when it evolves to have enough coverage and density.

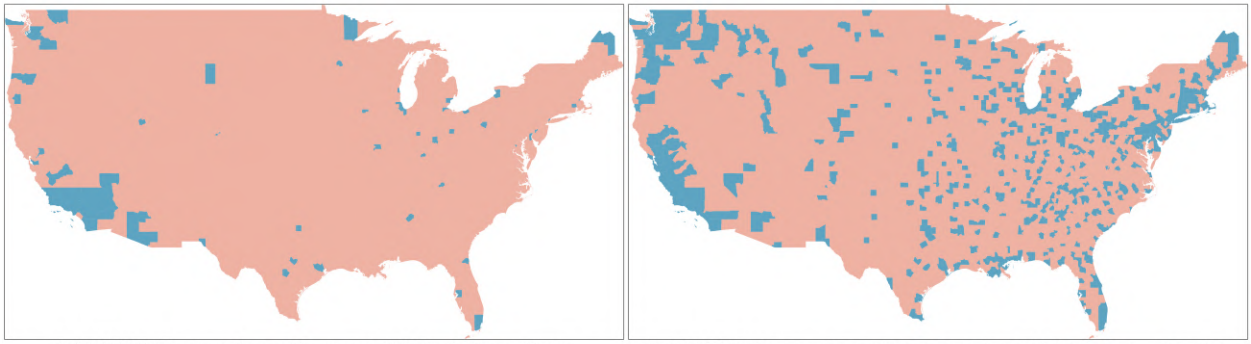

Figure 5: The contiguous U.S. counties in blue are those with a greater (a) number (∼2% of the total counties) or (b) density (∼20% of the total counties) of AQS $PM_{2.5}$ stations than Imperial County in 2017. The red areas are the potential regions in the U.S. where our proposed $PM_{2.5}$ prediction framework with low-cost sensor measurements can be applied to generate $PM_{2.5}$ spatial details.

5 Conclusions

With an exemplary low-cost air quality monitoring network in Imperial County, IVAN, we evaluated the contribution of low-cost sensor measurements to $PM_{2.5}$ prediction when regulatory measurements were insufficient to support reliable small-scale $PM_{2.5}$ modeling. This study proved that the integration of a large number of low-cost sensor measurements with sparse regulatory measurements is an effective way to improve the quality of $PM_{2.5}$ prediction significantly. This study also highlighted the needs of more effective calibration or integration methods to mitigate the negative impact caused by the remaining uncertainty in low-cost

sensor measurements on the prediction quality. This is the first study to report high-resolution $PM_{2.5}$ distributions in Imperial County by virtue of dense low-cost sensor measurements. The proposed $PM_{2.5}$ prediction framework with low-cost sensor measurements has enormous potential to be applied in vast areas worldwide with insufficient regulatory stations to identify $PM_{2.5}$ pollution details which are fundamental to $PM_{2.5}$-related health research.

Acknowledgments

The work of J. Bi, J. Stowell, and Y. Liu was supported by the National Aeronautics and Space Administration (NASA) Applied Sciences Program (Grant # NNX16AQ28Q and 80NSSC19K0191). The work of F. Freedman was supported by the NASA Applied Sciences Program (Grant # NNX16AQ91G). The work of P. English was supported by the National Institute of Environmental Health Sciences of the National Institutes of Health (NIH) (Grant # R01ES022722). The content is solely the responsibility of the authors and does not necessarily represent the official views of NASA and NIH.

The authors acknowledge the Imperial Valley Air Network (IVAN) team of researchers and stakeholders at Comite Civico Del Valle, Inc. lead by Luis Olmedo, Tracking California, and the University of Washington for providing and assisting us in utilizing the IVAN air monitoring data for this study. See https://ivan-imperial.org/ for more details about the IVAN monitoring program.

References

J. Bi, J. H. Belle, Y. Wang, A. I. Lyapustin, A. Wildani, and Y. Liu. Impacts of snow and cloud covers on satellite-derived pm2.5 levels. *Remote Sens Environ*, 221:665–674, 2019. ISSN 0034-4257 (Print) 0034-4257 (Linking). doi: 10.1016/j.rse.2018.12.002. URL https://www.ncbi.nlm.nih.gov/pubmed/31359889.

B. K. Blaylock, J. D. Horel, and S. T. Liston. Cloud archiving and data mining of high-resolution rapid refresh forecast model output. *Computers & Geosciences*, 109:43–50, 2017. ISSN 00983004. doi: 10.1016/j.cageo.2017.08.005.

S. Bose, N. N. Hansel, E. S. Tonorezos, D. L. Williams, A. Bilderback, P. N. Breysse, G. B. Diette, and M. C. McCormack. Indoor particulate matter associated with systemic inflammation in copd. *Journal of Environmental Protection*, 06(05):566–572, 2015. ISSN 2152-2197 2152-2219. doi: 10.4236/jep.2015.65051.

L. Breiman. Random forests. *Machine Learning*, 45(1):5–32, 2001. ISSN 08856125. doi: 10.1023/a:1010933404324. URL <GotoISI>://WOS:000170489900001.

D. M. Broday et al. Wireless distributed environmental sensor networks for air pollution measurement-the promise and the current reality. *Sensors (Basel)*, 17(10):2263, 2017. ISSN 1424-8220 (Electronic) 1424-8220 (Linking). doi: 10.3390/s17102263. URL https://www.ncbi.nlm.nih.gov/pubmed/28974042.

C. Brokamp, R. Jandarov, M. Hossain, and P. Ryan. Predicting daily urban fine particulate matter concentrations using a random forest model. *Environ Sci Technol*, 52(7):4173–4179, 2018. ISSN 1520-5851 (Electronic) 0013-936X (Linking). doi: 10.1021/acs.est.7b05381. URL https://www.ncbi.nlm.nih.gov/pubmed/29537833.

R. T. Burnett, r. Pope, C. A., M. Ezzati, C. Olives, S. S. Lim, S. Mehta, H. H. Shin, G. Singh, B. Hubbell, M. Brauer, H. R. Anderson, K. R. Smith, J. R. Balmes, N. G. Bruce, H. Kan, F. Laden, A. Pruss-Ustun, M. C. Turner, S. M. Gapstur, W. R. Diver, and A. Cohen. An integrated risk function for estimating the global burden of disease attributable to ambient fine particulate matter exposure. *Environ Health Perspect*, 122(4):397–403, 2014. ISSN 1552-9924 (Electronic) 0091-6765 (Linking). doi: 10.1289/ehp.1307049. URL https://www.ncbi.nlm.nih.gov/pubmed/24518036.

T. Cao and J. E. Thompson. Portable, ambient pm2.5 sensor for human and/or animal exposure studies. *Analytical Letters*, 50(4):712–723, 2017. ISSN 0003-2719.

CARB. Air quality trends summaries. California Air Resources Board, 2017. URL https://www.arb.ca.gov/adam/trends/trends1.php.

G. N. Carvlin, H. Lugo, L. Olmedo, E. Bejarano, A. Wilkie, D. Meltzer, M. Wong, G. King, A. Northcross, M. Jerrett, P. B. English, D. Hammond, and E. Seto. Development and field validation of a community-engaged particulate matter air quality monitoring network in imperial, california, usa. *J Air Waste Manag Assoc*, 67(12):1342–1352, 2017. ISSN 2162-2906 (Electronic) 1096-2247 (Linking). doi: 10.1080/10962247.2017.1369471. URL https://www.ncbi.nlm.nih.gov/pubmed/28829718.

N. Castell, F. R. Dauge, P. Schneider, M. Vogt, U. Lerner, B. Fishbain, D. Broday, and A. Bartonova. Can commercial low-cost sensor platforms contribute to air quality monitoring and exposure estimates? *Environment international*, 99:293–302, 2017. ISSN 0160-4120.

CEHTP. Emergency department visits due to asthma. California Environmental Health Tracking Program, 2018. URL http://www.cehtp.org/page/asthma/query.

J. C. Chow, J. G. Watson, M. C. Green, D. H. Lowenthal, B. Bates, W. Oslund, and G. Torres. Cross-border transport and spatial variability of suspended particles in mexicali and california's imperial valley. *Atmospheric environment*, 34(11):1833–1843, 2000. ISSN 1352-2310.

J. C. Chow, L. A. Chen, J. G. Watson, D. H. Lowenthal, K. A. Magliano, K. Turkiewicz, and D. E. Lehrman. Pm2.5 chemical composition and spatiotemporal variability during the california regional pm10/pm2.5 air quality study (crpaqs). *Journal of Geophysical Research: Atmospheres*, 111(D10), 2006. ISSN 2156-2202.

Y. Chu, Y. Liu, X. Li, Z. Liu, H. Lu, Y. Lu, Z. Mao, X. Chen, N. Li, and M. Ren. A review on predicting ground pm2.5 concentration using satellite aerosol optical depth. *Atmosphere*, 7(10):129, 2016.

Q. Di, I. Kloog, P. Koutrakis, A. Lyapustin, Y. Wang, and J. Schwartz. Assessing pm2.5 exposures with high spatiotemporal resolution across the continental united states. *Environ Sci Technol*, 50(9):4712–21, 2016. ISSN 1520-5851 (Electronic) 0013-936X (Linking). doi: 10.1021/acs.est.5b06121. URL https://www.ncbi.nlm.nih.gov/pubmed/27023334.

P. B. English, L. Olmedo, E. Bejarano, H. Lugo, E. Murillo, E. Seto, M. Wong, G. King, A. Wilkie, D. Meltzer, G. Carvlin, M. Jerrett, and A. Northcross. The imperial county community air monitoring network: A model for community-based environmental monitoring for public health action. *Environ Health Perspect*, 125(7):074501, 2017. ISSN 1552-9924 (Electronic) 0091-6765 (Linking). doi: 10.1289/EHP1772. URL https://www.ncbi.nlm.nih.gov/pubmed/28886604.

C. Garzón-Galvis, M. Wong, D. Madrigal, L. Olmedo, M. Brown, and P. English. *Advancing Environmental Health Literacy Through Community-Engaged Research and Popular Education*, pages 97–134. Springer, 2019.

G. Geng, N. L. Murray, H. H. Chang, and Y. Liu. The sensitivity of satellite-based pm2.5 estimates to its inputs: Implications to model development in data-poor regions. *Environ Int*, 121(Pt 1):550–560, 2018a. ISSN 1873-6750 (Electronic) 0160-4120 (Linking). doi: 10.1016/j.envint.2018.09.051. URL https://www.ncbi.nlm.nih.gov/pubmed/30300813.

G. Geng, N. L. Murray, D. Tong, J. S. Fu, X. Hu, P. Lee, X. Meng, H. H. Chang, and Y. Liu. Satellite-based daily pm2.5 estimates during fire seasons in colorado. *J Geophys Res Atmos*, 123(15):8159–8171, 2018b. ISSN 2169-897X (Print) 2169-897X (Linking). doi: 10.1029/2018JD028573. URL https://www.ncbi.nlm.nih.gov/pubmed/31289705.

E. S. Hall, S. M. Kaushik, R. W. Vanderpool, R. M. Duvall, M. R. Beaver, R. W. Long, and P. A. Solomon. Integrating sensor monitoring technology into the current air pollution regulatory support paradigm: Practical considerations. *American Journal of Environmental Engineering*, 4(6):147–154, 2014. ISSN 2166-465X.

D. M. Holstius, A. Pillarisetti, K. Smith, and E. Seto. Field calibrations of a low-cost aerosol sensor at a regulatory monitoring site in california. *Atmospheric Measurement Techniques*, 7(4):1121–1131, 2014. ISSN 1867-1381.

X. Hu, L. A. Waller, A. Lyapustin, Y. Wang, M. Z. Al-Hamdan, W. L. Crosson, M. G. Estes, S. M. Estes, D. A. Quattrochi, S. J. Puttaswamy, and Y. Liu. Estimating ground-level pm2.5 concentrations in the southeastern united states using maiac aod retrievals and a two-stage model. *Remote Sensing of Environment*, 140:220–232, 2014. ISSN 00344257. doi: 10.1016/j.rse.2013.08.032. URL <GotoISI>://WOS:000329766200019.

X. Hu, J. H. Belle, X. Meng, A. Wildani, L. A. Waller, M. J. Strickland, and Y. Liu. Estimating pm2.5 concentrations in the conterminous united states using the random forest approach. *Environ Sci Technol*, 51(12):6936–6944, 2017. ISSN 1520-5851 (Electronic) 0013-936X (Linking). doi: 10.1021/acs.est.7b01210. URL https://www.ncbi.nlm.nih.gov/pubmed/28534414.

M. Jerrett, A. Arain, P. Kanaroglou, B. Beckerman, D. Potoglou, T. Sahsuvaroglu, J. Morrison, and C. Giovis. A review and evaluation of intraurban air pollution exposure models. *J Expo Anal Environ Epidemiol*, 15(2):185–204, 2005. ISSN 1053-4245 (Print) 1053-4245 (Linking). doi: 10.1038/sj.jea.7500388. URL https://www.ncbi.nlm.nih.gov/pubmed/15292906.

W. Jiao, G. Hagler, R. Williams, R. Sharpe, R. Brown, D. Garver, R. Judge, M. Caudill, J. Rickard, and M. Davis. Community air sensor network (cairsense) project: evaluation of low-cost sensor performance in a suburban environment in the southeastern united states. *Atmospheric Measurement Techniques*, 9 (11):5281–5292, 2016. ISSN 1867-1381.

A. C. Just, R. O. Wright, J. Schwartz, B. A. Coull, A. A. Baccarelli, M. M. Tellez-Rojo, E. Moody, Y. Wang, A. Lyapustin, and I. Kloog. Using high-resolution satellite aerosol optical depth to estimate daily pm2.5 geographical distribution in mexico city. *Environ Sci Technol*, 49(14):8576–84, 2015. ISSN 1520-5851 (Electronic) 0013-936X (Linking). doi: 10.1021/acs.est.5b00859. URL https://www.ncbi.nlm.nih.gov/pubmed/26061488.

K. E. Kelly, J. Whitaker, A. Petty, C. Widmer, A. Dybwad, D. Sleeth, R. Martin, and A. Butterfield. Ambient and laboratory evaluation of a low-cost particulate matter sensor. *Environ Pollut*, 221:491–500, 2017. ISSN 1873-6424 (Electronic) 0269-7491 (Linking). doi: 10.1016/j.envpol.2016.12.039. URL https://www.ncbi.nlm.nih.gov/pubmed/28012666.

J. King, V. Etyemezian, M. Sweeney, B. J. Buck, and G. Nikolich. Dust emission variability at the salton sea, california, usa. *Aeolian Research*, 3(1):67–79, 2011. ISSN 1875-9637.

I. Kloog, P. Koutrakis, B. A. Coull, H. J. Lee, and J. Schwartz. Assessing temporally and spatially resolved pm2.5 exposures for epidemiological studies using satellite aerosol optical depth measurements. *Atmospheric Environment*, 45(35):6267–6275, 2011. ISSN 13522310. doi: 10.1016/j.atmosenv.2011.08.066. URL <GotoISI>://WOS:000295653800001.

A. Liaw and M. Wiener. Classification and regression by randomforest. *R news*, 2(3):18–22, 2002. ISSN 1609-3631.

Y. Liu, R. J. Park, D. J. Jacob, Q. Li, V. Kilaru, and J. A. Sarnat. Mapping annual mean ground-level pm2.5 concentrations using multiangle imaging spectroradiometer aerosol optical thickness over the contiguous united states. *Journal of Geophysical Research: Atmospheres*, 109(D22), 2004. ISSN 0148-0227.

Z. Ma, X. Hu, A. M. Sayer, R. Levy, Q. Zhang, Y. Xue, S. Tong, J. Bi, L. Huang, and Y. Liu. Satellite-based spatiotemporal trends in pm2.5 concentrations: China, 2004-2013. *Environ Health Perspect*, 124 (2):184–92, 2016. ISSN 1552-9924 (Electronic) 0091-6765 (Linking). doi: 10.1289/ehp.1409481. URL https://www.ncbi.nlm.nih.gov/pubmed/26220256.

J. Madrigano, I. Kloog, R. Goldberg, B. A. Coull, M. A. Mittleman, and J. Schwartz. Long-term exposure to pm2.5 and incidence of acute myocardial infarction. *Environ Health Perspect*, 121(2):192–6, 2013. ISSN

1552-9924 (Electronic) 0091-6765 (Linking). doi: 10.1289/ehp.1205284. URL https://www.ncbi.nlm.nih.gov/pubmed/23204289.

L. Morawska, P. K. Thai, X. Liu, A. Asumadu-Sakyi, G. Ayoko, A. Bartonova, A. Bedini, F. Chai, B. Christensen, and M. Dunbabin. Applications of low-cost sensing technologies for air quality monitoring and exposure assessment: How far have they gone? *Environment international*, 116:286–299, 2018. ISSN 0160-4120.

C. J. Paciorek, Y. Liu, H. Moreno-Macias, and S. Kondragunta. Spatiotemporal associations between goes aerosol optical depth retrievals and ground-level pm2.5. *Environmental science & technology*, 42(15): 5800–5806, 2008. ISSN 0013-936X.

S. P. Parajuli and C. S. Zender. Projected changes in dust emissions and regional air quality due to the shrinking salton sea. *Aeolian Research*, 33:82–92, 2018. ISSN 1875-9637.

W. F. Rogge, P. M. Medeiros, and B. R. Simoneit. Organic marker compounds for surface soil and fugitive dust from open lot dairies and cattle feedlots. *Atmospheric Environment*, 40(1):27–49, 2006. ISSN 1352-2310.

P. E. Saide, G. R. Carmichael, S. N. Spak, L. Gallardo, A. E. Osses, M. A. Mena-Carrasco, and M. Pagowski. Forecasting urban pm10 and pm2.5 pollution episodes in very stable nocturnal conditions and complex terrain using wrf–chem co tracer model. *Atmospheric Environment*, 45(16):2769–2780, 2011. ISSN 1352-2310.

E. G. Snyder, T. H. Watkins, P. A. Solomon, E. D. Thoma, R. W. Williams, G. S. Hagler, D. Shelow, D. A. Hindin, V. J. Kilaru, and P. W. Preuss. The changing paradigm of air pollution monitoring. *Environ Sci Technol*, 47(20):11369–77, 2013. ISSN 1520-5851 (Electronic) 0013-936X (Linking). doi: 10.1021/es4022602. URL https://www.ncbi.nlm.nih.gov/pubmed/23980922.

M. Sorek-Hamer, A. C. Just, and I. Kloog. Satellite remote sensing in epidemiological studies. *Curr Opin Pediatr*, 28(2):228–34, 2016. ISSN 1531-698X (Electronic) 1040-8703 (Linking). doi: 10.1097/MOP.0000000000000326. URL https://www.ncbi.nlm.nih.gov/pubmed/26859287.

A. van Donkelaar, R. V. Martin, and R. J. Park. Estimating ground-level pm2.5 using aerosol optical depth determined from satellite remote sensing. *Journal of Geophysical Research: Atmospheres*, 111(D21), 2006. ISSN 2156-2202.

A. van Donkelaar, R. V. Martin, M. Brauer, R. Kahn, R. Levy, C. Verduzco, and P. J. Villeneuve. Global estimates of ambient fine particulate matter concentrations from satellite-based aerosol optical depth: development and application. *Environ Health Perspect*, 118(6):847–55, 2010. ISSN 1552-9924 (Electronic) 0091-6765 (Linking). doi: 10.1289/ehp.0901623. URL https://www.ncbi.nlm.nih.gov/pubmed/20519161.

W. Wang, F. Mao, L. Du, Z. Pan, W. Gong, and S. Fang. Deriving hourly pm2.5 concentrations from himawari-8 aods over beijing–tianjin–hebei in china. *Remote Sensing*, 9(8):858, 2017.

Y. Wang, J. Li, H. Jing, Q. Zhang, J. Jiang, and P. Biswas. Laboratory evaluation and calibration of three low-cost particle sensors for particulate matter measurement. *Aerosol Science and Technology*, 49(11): 1063–1077, 2015. ISSN 0278-6826.

S. C. Wilson, J. Morrow-Tesch, D. C. Straus, J. D. Cooley, W. C. Wong, F. M. Mitlohner, and J. J. McGlone. Airborne microbial flora in a cattle feedlot. *Appl Environ Microbiol*, 68(7):3238–42, 2002. ISSN 0099-2240 (Print) 0099-2240 (Linking). doi: 10.1128/aem.68.7.3238-3242.2002. URL https://www.ncbi.nlm.nih.gov/pubmed/12088999.

M. Wong, E. Bejarano, G. Carvlin, K. Fellows, G. King, H. Lugo, M. Jerrett, D. Meltzer, A. Northcross, L. Olmedo, E. Seto, A. Wilkie, and P. English. Combining community engagement and scientific approaches in next-generation monitor siting: The case of the imperial county community air network. *Int J Environ Res Public Health*, 15(3):523, 2018. ISSN 1660-4601 (Electronic) 1660-4601 (Linking). doi: 10.3390/ijerph15030523. URL https://www.ncbi.nlm.nih.gov/pubmed/29543726.

Q. Xiao, Y. Wang, H. H. Chang, X. Meng, G. Geng, A. Lyapustin, and Y. Liu. Full-coverage high-resolution daily pm 2.5 estimation using maiac aod in the yangtze river delta of china. *Remote Sensing of Environment*, 199:437–446, 2017. ISSN 00344257. doi: 10.1016/j.rse.2017.07.023. URL <GotoISI>://WOS:000410469100033.

Q. Xiao, H. H. Chang, G. Geng, and Y. Liu. An ensemble machine-learning model to predict historical pm2.5 concentrations in china from satellite data. *Environ Sci Technol*, 52(22):13260–13269, 2018. ISSN 1520-5851 (Electronic) 0013-936X (Linking). doi: 10.1021/acs.est.8b02917. URL https://www.ncbi.nlm.nih.gov/pubmed/30354085.

R. Xu. *Particle characterization: light scattering methods*, volume 13. Springer Science & Business Media, 2001. ISBN 1402003579.

S. L. Zeger, D. Thomas, F. Dominici, J. M. Samet, J. Schwartz, D. Dockery, and A. Cohen. Exposure measurement error in time-series studies of air pollution: concepts and consequences. *Environ Health Perspect*, 108(5):419–26, 2000. ISSN 0091-6765 (Print) 0091-6765 (Linking). doi: 10.1289/ehp.00108419. URL https://www.ncbi.nlm.nih.gov/pubmed/10811568.

B. Zou, M. Wang, N. Wan, J. G. Wilson, X. Fang, and Y. Tang. Spatial modeling of pm2.5 concentrations with a multifactoral radial basis function neural network. *Environ Sci Pollut Res Int*, 22(14):10395–404, 2015. ISSN 1614-7499 (Electronic) 0944-1344 (Linking). doi: 10.1007/s11356-015-4380-3. URL https://www.ncbi.nlm.nih.gov/pubmed/25813644.

Supplementary Material

1. Daily Aggregation of IVAN Measurements

In this study, soft criteria were adopted for the aggregation of hourly IVAN measurements into daily data. Specifically, all available hourly measurements were used for aggregation without concerning the hourly coverage. IVAN is a well-maintained low-cost sensor network. Before the daily aggregation, the completeness and continuity of IVAN hourly measurements were examined. We found that the sensors had very high hourly coverage during the study period. The mean coverage of each site in each day was > 22 hours with an interquartile range of 0 (median: 24 hours; 25% and 75% percentiles: 24 hours). Only < 3% of the sensor-days (the total days during the study period multiplies the number of sensors) had the hourly coverage < 5 hours. Although this small number of daily measurements aggregated from < 5 hourly measurements might bias the predictions at the daily level, this uncertainty may have limited influence on our major conclusions which were mainly based on the overall prediction pattern during the study period.

2. AOD Missingness and Gap-Filling

Satellite AOD has a large proportion of missing retrievals over land due to cloud cover and high surface brightness (*e.g.,* standing water). Missing AOD retrievals have significantly hindered the generation of fully-covered $PM_{2.5}$ estimates. Recent studies overcome this obstacle by estimating missing AOD data before predicting $PM_{2.5}$, a process called AOD gap-filling (Bi et al. 2019; Li et al. 2012; Van Donkelaar et al. 2011; Xiao et al. 2017). In this study, we followed the approach proposed by Bi et al. (2019) to conduct AOD gap-filling, in which random forest models with AOD-related predictors were established at a daily level. The predictors consisted of 1) cloud fraction, 2) 2-meter specific humidity, 3) 2-meter temperature, 4) planetary boundary layer height, 5) surface wind speed, and 6) spatial coordinates of AOD retrievals. The AOD gap-filling was separately conducted for Terra and Aqua datasets. A three-day moving time window was applied to increase the sample size (Xiao et al. 2017). As in Bi et al. (2019), the random forest-specific out-of-bag (OOB) R^2 and root-mean-square error (RMSE) were used to evaluate the performance of AOD gap-filling.

During the study period (September 2016 to November 2017), Terra AOD had a mean daily missing rate of 36.9% with an interquartile range (IQR) from 6.3% to 69.3%. Aqua AOD had a mean daily missing rate of 40.8% with an IQR from 8.0% to 76.3%. Figure S4 shows the patterns of missing AOD retrievals of Terra and Aqua during the study period. The grid cells over water bodies (*e.g.*, the Salton Sea) were filtered out (Chu et al. 2002). Besides water bodies, missing AOD was evenly distributed throughout the study domain with minor increases in the regions covered by dense vegetation. The gap-filling models had good performance with a mean OOB R^2 of 0.95 and a mean RMSE of 0.013 for both Terra and Aqua datasets. As in Xiao et al. (2017) and Bi et al. (2019), we also found that the gap-filled AOD values tended to be higher than the original AOD retrieved under clear-sky condition. Xiao et al. (2017) and Bi et al. (2019) suggested that this pattern may be caused by aerosol hygroscopic growth.

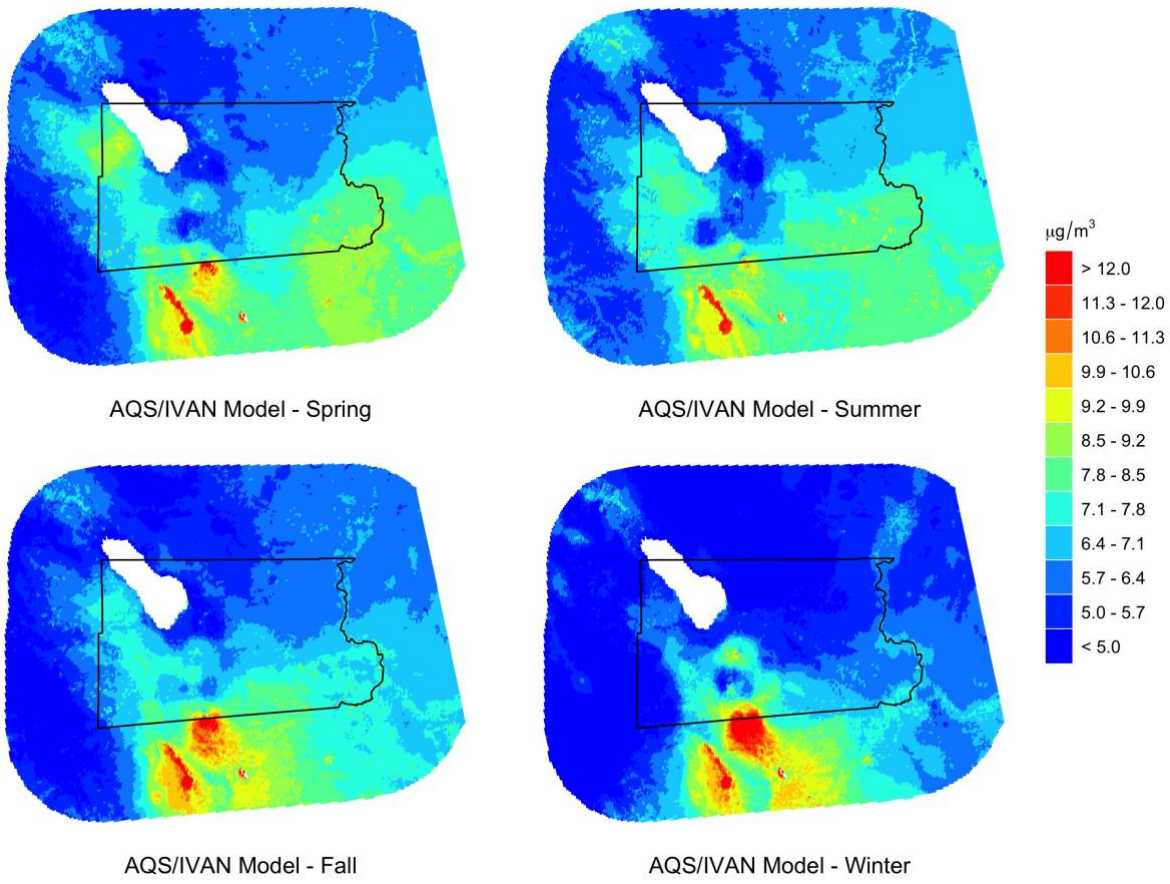

Figure S1 Mean $PM_{2.5}$ distributions in different seasons generated by the AQS/IVAN model during the study period.

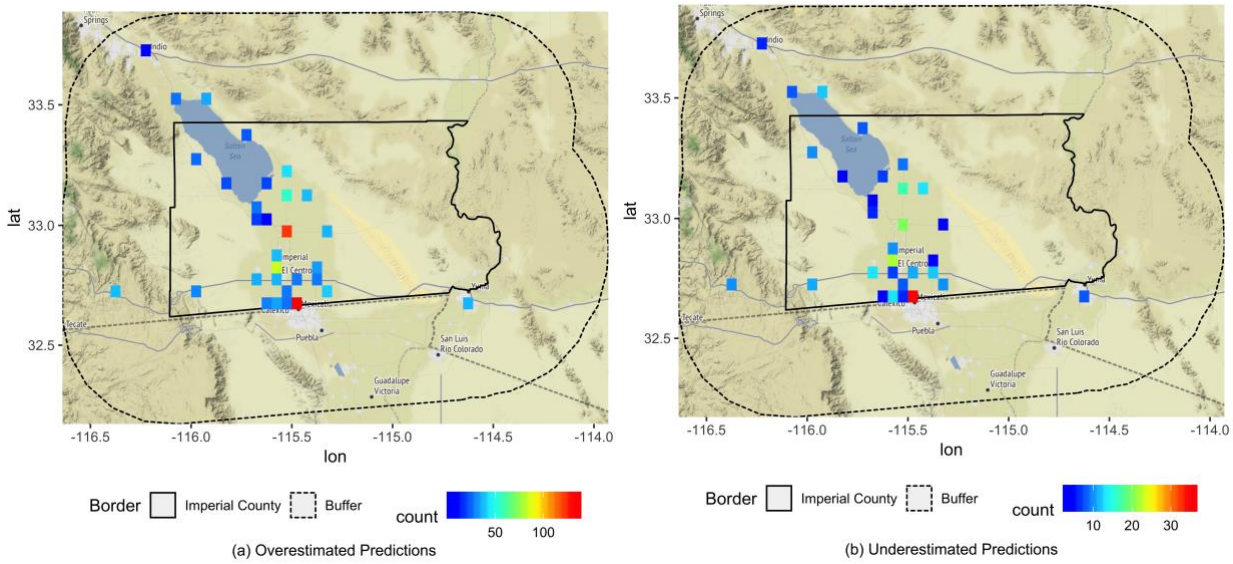

Figure S2 Frequencies of prediction outliers at the locations of AQS and IVAN stations (left: overestimated predictions; right: underestimated predictions).

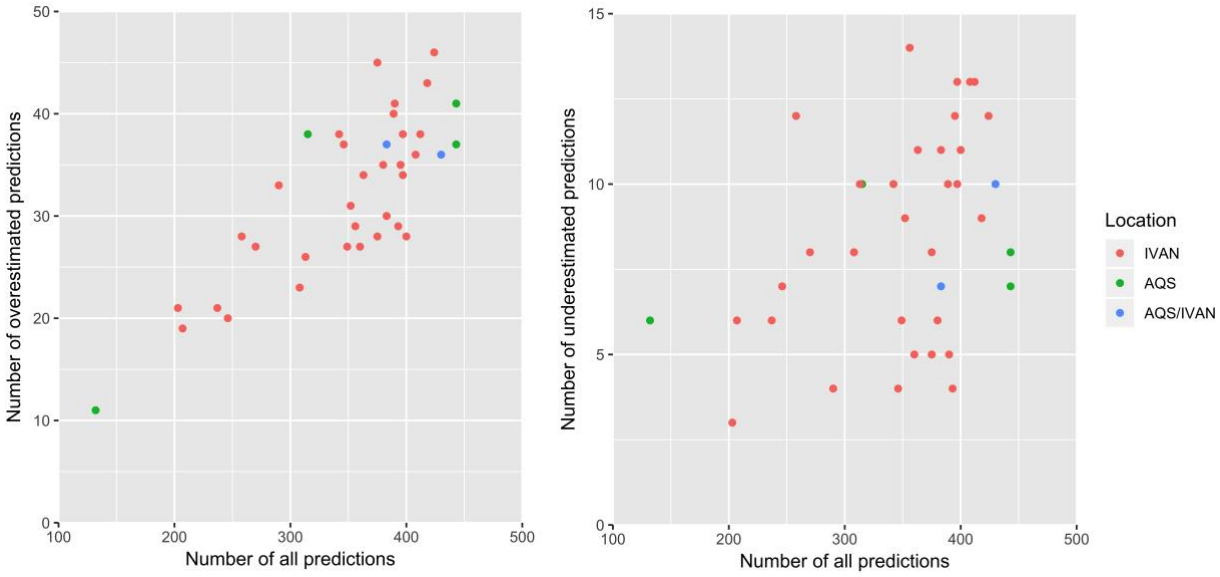

Figure S3 Correlations between the number of outliers and the number of predictions (left: overestimated predictions; right: underestimated predictions).

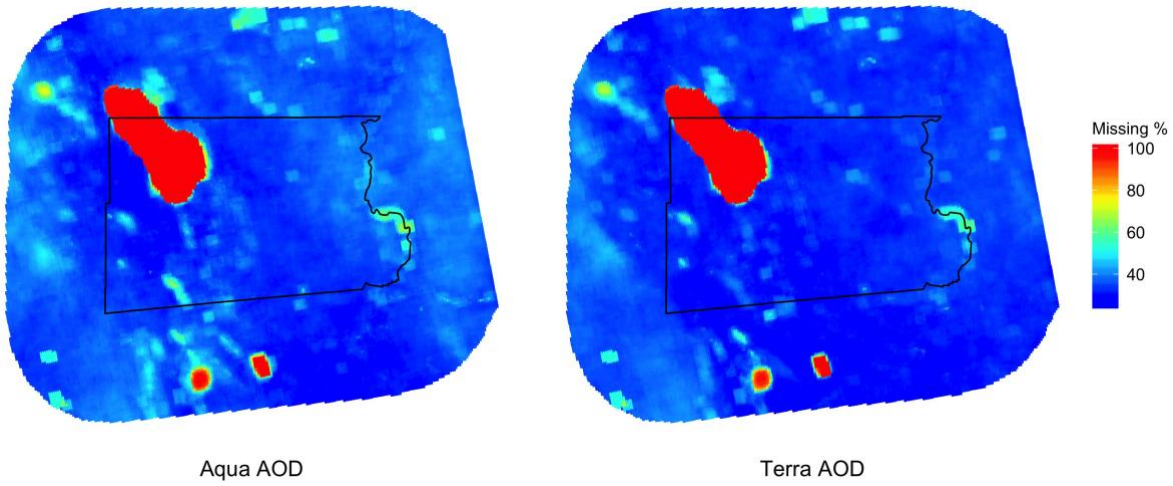

Figure S4 Distributions of the average missing rates of Terra/Aqua AOD during the study period.

References

Bi, J., Belle, J.H., Wang, Y., Lyapustin, A.I., Wildani, A., & Liu, Y. (2019). Impacts of snow and cloud covers on satellite-derived PM2.5 levels. *Remote Sensing of Environment, 221*, 665-674

Chu, D.A., Kaufman, Y.J., Ichoku, C., Remer, L.A., Tanre, D., & Holben, B.N. (2002). Validation of MODIS aerosol optical depth retrieval over land. *Geophysical Research Letters, 29*

Li, S., Chen, L., Tao, J., Han, D., Wang, Z., Su, L., Fan, M., & Yu, C. (2012). Retrieval of aerosol optical depth over bright targets in the urban areas of North China during winter. *Science China Earth Sciences, 55*, 1545-1553

Van Donkelaar, A., Martin, R.V., Levy, R.C., da Silva, A.M., Krzyzanowski, M., Chubarova, N.E., Semutnikova, E., & Cohen, A.J. (2011). Satellite-based estimates of ground-level fine particulate matter during extreme events: A case study of the Moscow fires in 2010. *Atmospheric Environment, 45*, 6225-6232

Xiao, Q.Y., Wang, Y.J., Chang, H.H., Meng, X., Geng, G.N., Lyapustin, A., & Liu, Y. (2017). Full-coverage high-resolution daily PM2.5 estimation using MAIAC AOD in the Yangtze River Delta of China. *Remote Sensing of Environment, 199*, 437-446